COMBINED FORMALDEHYDE AND GLYOXAL OBSERVATIONS FROM GOME-2 BACKSCATTERED LIGHT MEASUREMENTS.

Christophe Lerot[(1)], Isabelle De Smedt[(1)], Trissevgeni Stavrakou[(1)], Jean-François Müller[(1)], and Michel Van Roozendael[(1)]

[(1)]Belgian Institute for Space Aeronomy (BIRA-IASB),3 Avenue circulaire, B-1180 Brussels (Belgium), christl@oma.be

ABSTRACT

Glyoxal (CHOCHO) and formaldehyde (HCHO) are short-lived intermediate products in the oxidation of non-methane volatile organic compounds (NMVOCs) emitted by vegetation, fires and anthropogenic activities. They are also directly emitted during fossil fuel and biofuel combustion and biomass burning. Both compounds absorb in the UV-visible spectral region which can be used for total column retrieval using the Differential Optical Absorption Spectroscopy (DOAS) technique. However, such measurements remain challenging mainly due to the overall faintness of the CHOCHO and HCHO signals, but also due to uncertainties in the calculation of air mass factors (AMFs).

Launched in October 2006 on board of METOP-A platform, the GOME-2 instrument measures the sunlight backscattered by the Earth's atmosphere between 240 nm and 790 nm, with a ground resolution of 80 km x 40 km. Compared to its predecessors GOME/ERS-2 and SCIAMACHY/ENVISAT, GOME-2 is characterized by a larger scan-width of 1920 km allowing for daily quasi-global coverage and therefore for a much better identification of local NMVOC emissions.

In this work, we present results of glyoxal and formaldehyde vertical columns from two years of GOME-2 observations (2007 and 2008). We compare the global observations of these two compounds as well as their seasonalities. Specific attention is given to East Asia, where anthropogenic emissions in the rapidly growing megacities are important. The synergistic use of glyoxal and formaldehyde observations offers the potential to provide better constraints to anthropogenic NMVOC emissions using inverse modeling techniques.

1. INTRODUCTION

It is estimated that 60% of the formaldehyde (HCHO) content in the troposphere is formed by the photochemical oxidation of methane. In addition, the oxidation of biogenic and anthropogenic non-methane volatile organic compounds (NMVOC) significantly contributes to the HCHO formation. Also, formaldehyde is directly emitted from biomass burning and from fossil fuel and biofuel combustion. Besides methane oxidation, the precursors of formaldehyde also generate glyoxal (CHOCHO). The a priori global production of formaldehyde and glyoxal, as estimated in [1,2], is given in Fig. 1.

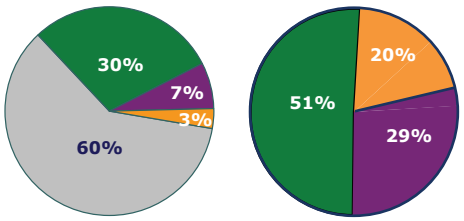

Figure 1: A priori global production of formaldehyde (left) and glyoxal (right). Production from methane oxidation is in grey, from biogenic precursors in green, from anthropogenic precursors in purple and from biomass burning in orange.

As the tropospheric lifetime of these two species is limited to a few hours, they are good proxy for NMVOC emissions. The potential of spaceborne formaldehyde and glyoxal measurements to constraint the parent NMVOC emissions has been demonstrated in a number of inverse modeling studies [1, 3-6]. Also, the ratio of glyoxal to formaldehyde amounts is a useful tool to characterize the impact of VOC emissions on tropospheric chemistry [7,8]. In addition, glyoxal is a significant source for secondary organic aerosols [9,10]. Thus, these measurements provide useful constraints for the establishment of their global budget.

Here, we focus on the formaldehyde and glyoxal vertical columns measured using the GOME-2/METOP-A nadir observations. This instrument [11] measures the sunlight backscattered by the Earth's atmosphere between 240 nm and 790 nm since October 2006. GOME-2 is characterized by a ground resolution of 80 km x 40 km and by a global coverage realized in 1.5 day. As the global coverage of its predecessors GOME and SCIAMACHY is poorer (respectively realized in 3 and 6 days), GOME-2 is expected to allow for a better identification of the local emissions and of their spatial structures.

Proc. 'Atmospheric Science Conference', Barcelona, Spain, 7–11 September 2009 (ESA SP-676, November 2009)

2. DOAS RETRIEVALS

To retrieve vertical columns of formaldehyde and glyoxal from GOME-2 measurements, the DOAS (Differential Optical Absorption Spectroscopy) technique is applied [12]. The retrieval is done in two different steps. First, a slant column (concentration integrated along the mean photon path) is retrieved using the structured absorption bands of the specie under study. Second, the slant column is converted into a vertical column using calculated air mass factors.

As illustrated in Fig. 2, formaldehyde and glyoxal have structured absorption bands in the ultra-violet and visible regions, respectively. For the DOAS retrievals, the formaldehyde fitting window is comprised between 328.5 nm and 346 nm while the corresponding interval for glyoxal is between 435 nm and 460 nm. The reference irradiance spectrum used in the DOAS fit is the solar spectrum daily measured by GOME-2. Other species absorb light in the HCHO and CHOCHO fitting windows and have to be taken into account in the DOAS fits. To retrieve HCHO slant columns, we include formaldehyde, ozone (at 228°K and 243°K), BrO, NO_2 and OClO cross-sections. To improve the quality of the fit at high solar zenith angles, BrO absorption is fixed to a value previously retrieved in a larger window (328.5-359 nm). In addition, a 2D-AMF table (wavelength, SZA) is applied to the ozone cross-sections during the formaldehyde retrieval. For glyoxal, we include CHOCHO, ozone, NO_2, H_2O, O_4, and liquid water cross-sections. The Ring effect [13] is treated as a pseudo-absorber for which a calculated spectrum is also included in the fit [14].

To calculate the air mass factors, look-up tables of altitude-resolved scattering weights have been generated (at 340 nm for HCHO and 448 nm for CHOCHO) using the radiative transfer model DISORT [15]. These look-up tables have 6 dimensions in order to consider the main parameters having an impact on the scattering weights (geometry, albedo and altitude of the reflecting surface). The air mass factor calculation also requires the a priori knowledge of the vertical concentration profile shape. These a priori profiles are provided by the Chemical Transport Model IMAGES v2 [1] with a spatial resolution of 2° x 2.5° (Lat. x Long.) and a 1-month time resolution. Although the pixels with large cloud fraction (>0.4) are filtered out, a cloud correction is applied based on the independent pixel approximation and using the FRESCO cloud parameters [16] provided in the level-1 data. Also, it has to be noted that no explicit correction for aerosols is applied.

Finally, a daily normalisation procedure is applied for all measurements using the reference sector method. This normalisation is based on the measurements in the Pacific ocean. For formaldehyde, it ensures that the columns measured in this sector are in good agreement with the HCHO background simulated by the model. For glyoxal, the normalization is realized so that the mean glyoxal column in the reference sector is equal to $2x10^{14}$ molec/cm². This normalization procedure is needed to correct for offsets introduced by the irradiance spectrum measurements and also for unresolved spectral interferences between HCHO, O_3 and BrO [17,18].

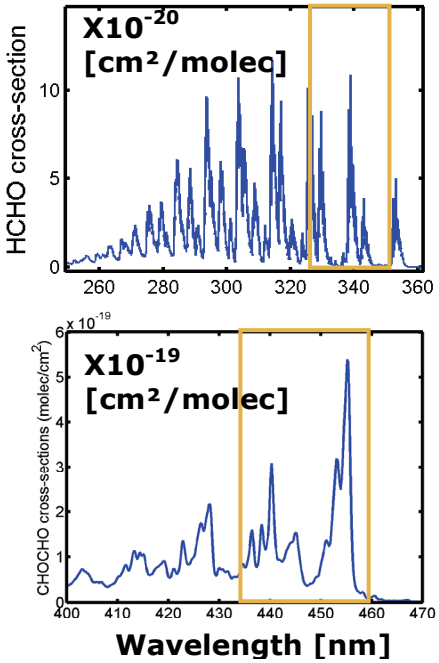

Figure 2: Absorption bands of formaldehyde in the UV (upper panel) and of glyoxal in the visible (lower panel). The regions used for the DOAS retrievals are highlighted by the yellow rectangle.

2.1. Glyoxal retrievals: Impact of liquid water absorption.

Fig. 3 (upper panel) shows the monthly mean glyoxal slant columns measured in December 2008 when the liquid water absorption is not considered. The glyoxal columns retrieved above remote oceans are systematically strongly negative. In addition, the quality of the DOAS fits in these regions is much poorer. This effect has already been observed in other studies based on SCIAMACHY or OMI data [19,20]. Fig. 4 shows the absorption cross-section of liquid water measured by Pope et al. [21]. A discontinuity is clearly visible in the glyoxal fitting interval and can not be filtered out by the DOAS polynomial closure term. If not explicitly considered, the liquid water absorption interferes with the glyoxal absorption leading to unphysical glyoxal slant columns for pixels over oceans. A correction for this is consequently needed. Unfortunately, because of these spectral interferences, the simultaneous adjustment of glyoxal and liquid water slant columns in the glyoxal retrievals also leads to unphysical results.

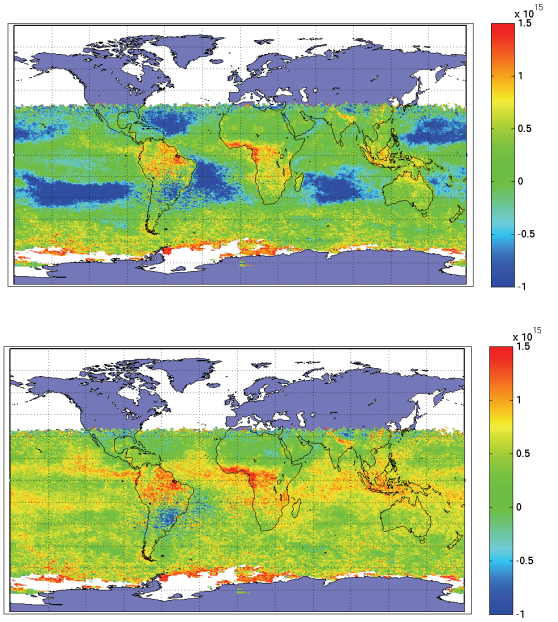

Figure 3: Monthly mean of the glyoxal slant columns retrieved in December 2008. The upper panel shows the columns retrieved without any correction for the liquid water absorption. The lower panel shows the columns retrieved when the liquid water absorption is considered in the DOAS fit.

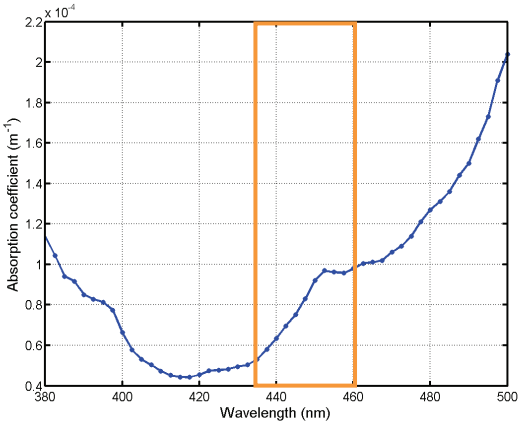

Figure 4: Liquid water absorption cross-section measured by Pope et al. [21]. A discontinuity is clearly visible in the glyoxal fitting window indicated by the yellow rectangle.

To consider the liquid water absorption in the glyoxal retrievals, a solution in two steps has been set up. First, an independent DOAS fit is used to measure the liquid water slant column. The fitting window for this retrieval is much wider (405 nm- 490 nm) in order to make use of the broad features of the liquid water cross-section. In this fit, only the ozone and O_4 cross-sections are considered in addition of the liquid water cross-section. Fig. 5 shows a map of the monthly mean liquid water slant columns retrieved in December 2008. High values are only measured over oceans where the glyoxal retrievals fail when the liquid water absorption is not considered. It is also important to note that the liquid water slant columns retrieved over lands are close to zero. After that step, the glyoxal slant column is retrieved by fixing the liquid water absorption to the value previously measured. This two-step method allows considering the liquid water absorption in the glyoxal fits with limited impact of spectral interferences. Fig. 3 (lower panel) shows the monthly mean glyoxal slant columns measured in December 2008 when the liquid water absorption is taken into account. It is clear that glyoxal columns over oceans are much more physical. Also, the DOAS fit quality in these regions is much higher. The impact of this correction on pixels over lands is relatively limited.

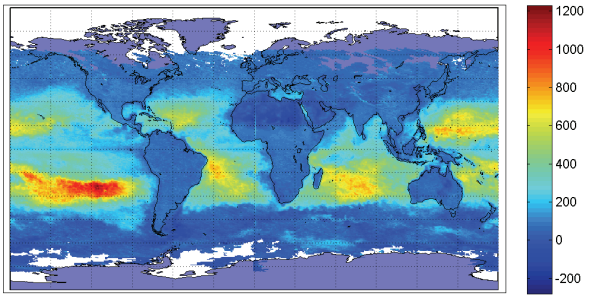

Figure 5: Monthly mean of the liquid water slant columns retrieved in December 2008.

2.2. Formaldehyde retrievals: consistency with GOME and SCIAMACHY.

Recently, the formaldehyde measurements from GOME and SCIAMACHY have been presented [18]. The good consistency between the two data sets was shown. Regarding the HCHO measurements from GOME-2, efforts have also been done to optimize the retrieval settings so as to obtain a consistent dataset based on the three instruments and covering almost 15 years. Fig. 6 illustrates the time series for two regions of the world. Compared to that of GOME and SCIAMACHY, the GOME-2 retrieval quality is poorer at mid-latitudes in winter due to the early overpass time of the instrument (9:30 am). Although attenuated by the aforementioned O_3 and BrO corrections, this effect has to be further investigated because it is worsened by the strong degradation of the instrument.

3. HCHO AND CHOCHO VERTICAL COLUMNS

Fig. 7 shows global views of the GOME-2 formaldehyde and glyoxal vertical columns averaged over different seasons. Although the formaldehyde concentrations are much higher than those of glyoxal, it is clear that the general features of the distribution of these two species are of the same kind due to

similarities in their source distributions. In general, the higher columns are found in Tropical Regions of Asia, Africa and South America where biogenic emissions are strong. Seasonal variations in the HCHO and CHOCHO fields following the emissions are also visible. As an illustration, the measured columns at mid-latitudes over Europe, the United States or Australia are significant during warm months and very small during the winter period. Unlike the formaldehyde columns, the glyoxal columns over the tropical oceans are high. The reason for this remains unclear. It might be due to local emissions in these biologically active regions or to the transport of glyoxal precursors from continental areas. This needs to be further examined.

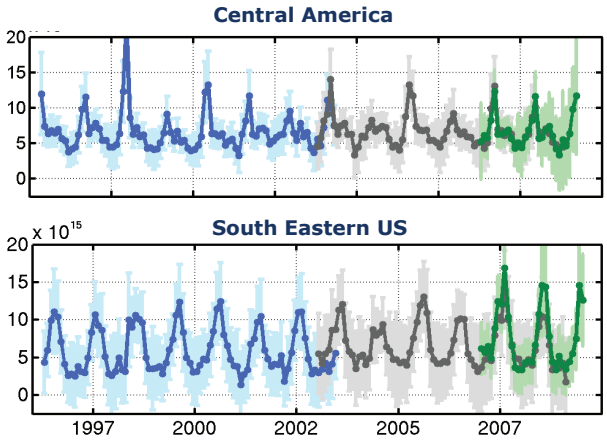

Figure 6: Illustration of the good consistency between the formaldehyde data sets retrieved from GOME (blue), SCIAMACHY (grey) and GOME-2 (green).

Fig. 8 focuses on Southeastern Asia and shows the mean vertical columns of formaldehyde and glyoxal for two different seasons. Again, the maps of these two compounds present the same general features. In addition, in this region where anthropogenic emissions are strong, hot spots are visible over several big cities, especially when the biogenic/pyrogenic emissions are weak. This is particularly the case with glyoxal probably due to high yields in the oxidation of anthropogenic VOCs. Consequently, a good indicator for anthropogenic emissions is the relatively high glyoxal columns associated with relatively low formaldehyde columns (as in the red-circled area of Fig. 8).

Fig. 9 shows time series of the monthly mean formaldehyde and glyoxal vertical columns in three different regions of Southeastern Asia. The seasonal dependencies of the two compounds are highly correlated illustrating that they respond in the same way to the seasonal variations of local emissions. Furthermore, the seasonal variations of formaldehyde and glyoxal can be strongly different from a location to another. Thus, the comparison of these data and of their spatial/temporal variabilities with columns calculated using a chemical transport model can help to better estimate the different categories of emission (see [1] for an example based on the SCIAMACHY measurements). From the a priori knowledge of the emissions, the large amplitude in the time variations observed in China is probably due to strong seasonal dependencies in the biogenic emissions. In Southeastern Asia, the amplitude of the seasonal variations in the vertical columns is even larger due to important biomass burning events. On the contrary, in India, the smaller time dependencies of HCHO and CHOCHO columns indicate that there is no strong variation in the local emissions.

4. FIRST COMPARISONS WITH GROUND-BASED DATA

A MAX-DOAS instrument has been installed by BIRA-IASB in Beijing between July 2008 and April 2009 to observe the possible impact of the measures taken to improve the air quality during the Olympic Games. Among other species, formaldehyde and glyoxal vertical columns have been retrieved from the MAX-DOAS spectra. On Fig. 10 the monthly mean HCHO and CHOCHO vertical columns from GOME-2 and from the ground-based instrument are compared. For these comparisons, only GOME-2 pixels lying within a radius of 100 km around the MAX-DOAS and only the ground-based data measured around the satellite overpass time have been considered. Although the ground-based air mass factors have been calculated in the geometrical approximation and could be further improved, we can nevertheless draw interesting conclusions. First, the order of magnitude of satellite-derived columns is consistent with that of the ground-based data for both products. Second, the GOME-2 HCHO columns tend to be too low in winter. Although the glyoxal measurements from GOME-2 and from the MAX-DOAS instrument are in good agreement (considering the error bars), the seasonality of ground-based glyoxal measurements is not well reproduced by the satellite data.

On the other hand, it is not straightforward to compare satellite data and ground-based measurements in Beijing. Indeed, Beijing is characterized by strong local emissions not necessarily captured by satellite measurements due to their low spatial resolution. In addition, Beijing is located at the foot of mountains. As illustrated in Fig. 11, the high glyoxal (and formaldehyde) vertical columns are concentrated in the valley while these columns are much lower over mountains. Consequently, there are strong spatial gradient in the formaldehyde and glyoxal fields around Beijing making the satellite – ground-based comparisons more difficult.

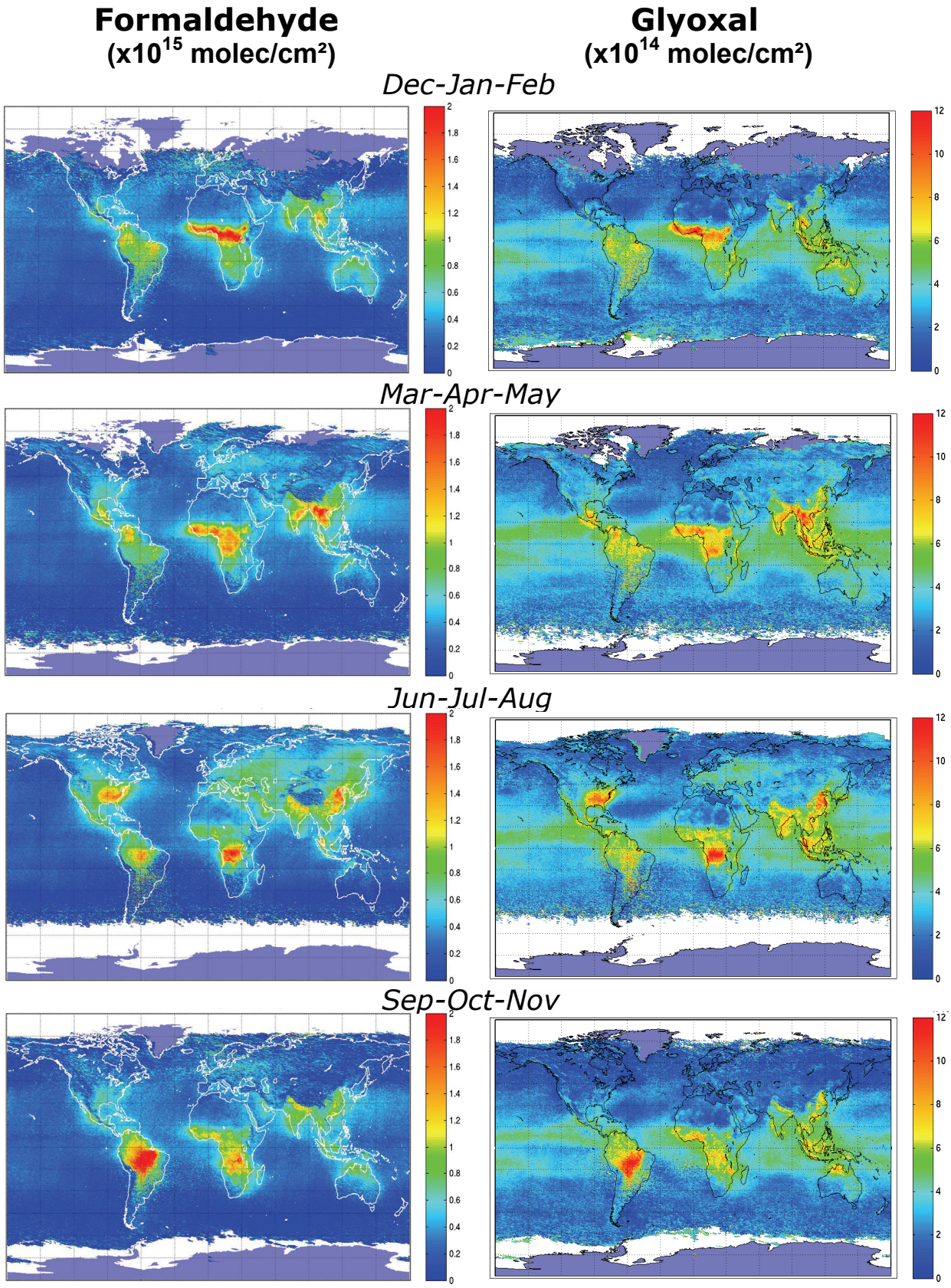

Figure 7: Global view of seasonally mean vertical columns of formaldehyde (left panels) and of glyoxal (right panel) measured from GOME-2 spectra.

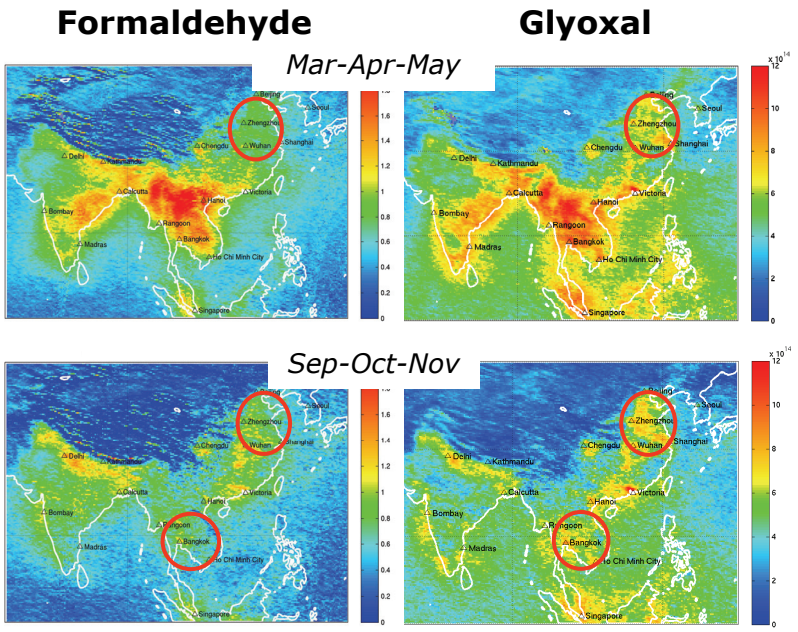

Figure 8: GOME-2 vertical columns of formaldehyde (left panels) and glyoxal (right panels) in Southeastern Asia in spring and autumn. The red circles show area where the glyoxal level is relatively high while the formaldehyde level is low. This is an indicator of anthropogenic emissions.

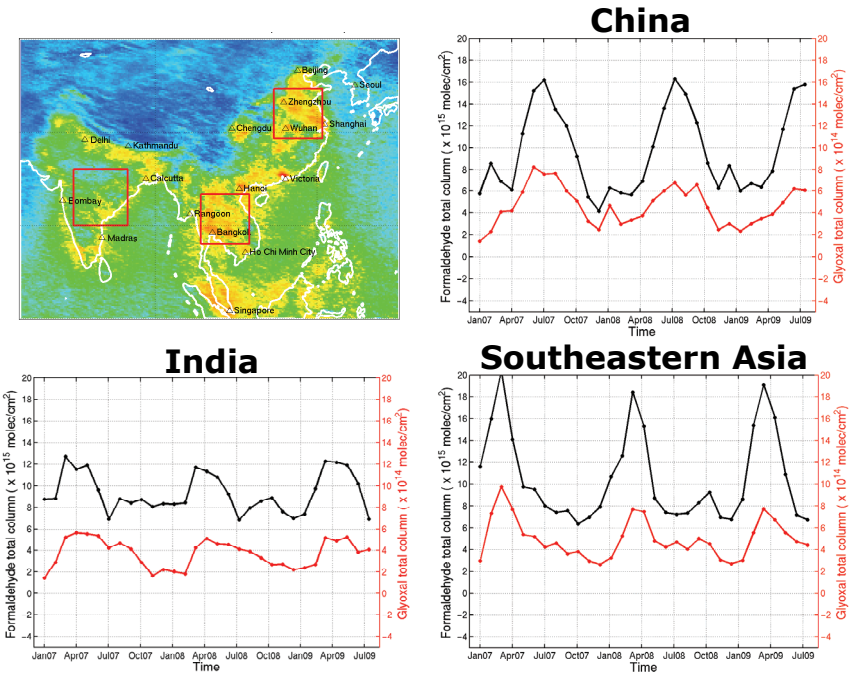

Figure 9: Time series of the monthly mean formaldehyde (black curve) and glyoxal (red curve) vertical columns in the three regions highlighted on the map (upper left panel). Note the different vertical scales for the two species.

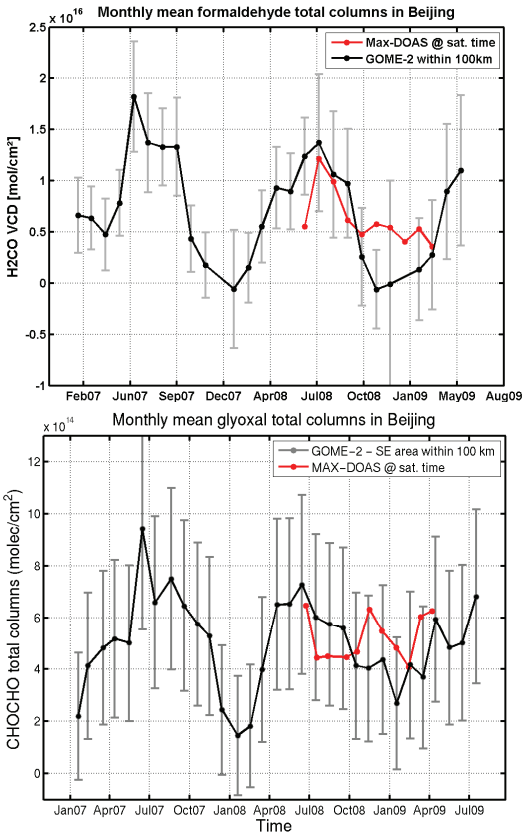

Figure 10: Comparisons of the monthly mean formaldehyde (upper panel) and glyoxal (lower panel) vertical columns measured by GOME-2 (black) with MAX-DOAS ground-based data (red) in Beijing.

5. SUMMARY AND PERSPECTIVES

In this paper, we have presented the algorithms developed at BIRA-IASB for retrieving the formaldehyde and glyoxal vertical columns using the GOME-2 observations. These algorithms are based on the DOAS technique that makes use of the structured absorption bands of formaldehyde and glyoxal in the ultra-violet and visible regions, respectively.
To measure the glyoxal columns over oceans, it is important to account for the liquid water absorption. For that, a two-step approach has been set up to minimize the impact of the spectral interferences between liquid water and glyoxal. It has also been shown that the GOME-2 measurements of formaldehyde vertical columns are very consistent with the GOME and SCIAMACHY datasets. Consequently, we have a combined formaldehyde data set covering 15 years so far.

Since formaldehyde and glyoxal have common sources, their spatial distributions are strongly correlated. The hot spots are generally found in Asia, Africa and South-America where biogenic emissions

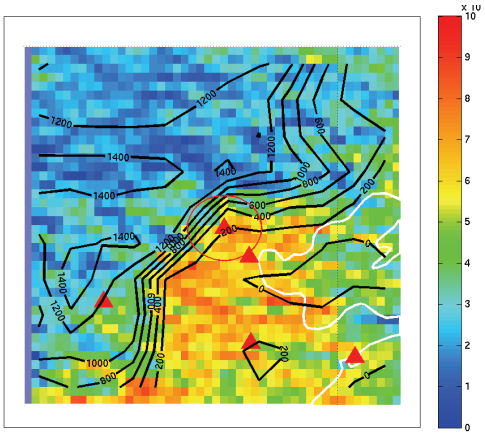

Figure 11: Glyoxal field in the Beijing area. The black curves represent the surface elevation contour lines. The red circle is centered on Beijing and has a radius of 100 km.

are important. Significant columns are also found at mid-latitudes during summer months. Seasonal variations of the formaldehyde and glyoxal columns have been observed and are obviously related to the temporal dependencies of the emissions.
The good coverage of the GOME-2 instrument allows for identification of anthropogenic emissions in these two data sets, especially in Asia where they are very strong. Finally, these formaldehyde and glyoxal vertical column measurements provide additional constraints on non-methane volatile organic compound emissions.

In the future, the possibly strong impact of aerosols has to be taken into account in the air mass factor calculations. Indeed, the aerosol loads in the troposphere can be very important over regions with high pyrogenic and anthropogenic emissions.
Despite the reasonable agreement between the GOME-2 and ground-based formaldehyde and glyoxal measurements in Beijing, a further validation of these products is needed (comparisons with other satellite products and with ground-based data).

Acknowledgements

This work was funded by the PROMOTE, TEMIS and AMFIC projects. The authors gratefully acknowledge the Institute of Atmospheric Physics, the Chinese Academy of Sciences (IAP/CAS) for the support to the MAX-DOAS measurements in Beijing.

6. REFERENCES

1. Stavrakou, T., Müller, J.-F., De Smedt, I., Van Roozendael, M., Kanakidou, M., Vrekoussis, M., Wittrock, F., Richter, A. & Burrows, J. (2009). The continental source of glyoxal estimated by the synergistic use of spaceborne measurements and

inverse modeling, *Atmos. Chem. Phys. Discuss.*, **9**, 13593-13628.
2. Stavrakou, T., Müller, J.-F., De Smedt, I., Van Roozendael, M., van der Werf, G.R., Giglio, L. & Guenther, A. (2009). Evaluating the performance of pyrogenic and biogenic emission inventories against one decade of space-based formaldehyde columns, *Atmos. Chem. Phys.,* **9**, 1037-1060.
3. Palmer, P. I., Jacob, D. J., Fiore, A. M., Martin, R. V., Chance, K., & Kurosu, T. P. (2003). Mapping isoprene emissions over North America using formaldehyde column observations from space, *J. Geophys. Res.*, **108**, D6, 4180, doi: 10,1029/2002JD002153.
4. Palmer, P. I., Abbot, D. S., Fu, T.-M., Jacob, D. J., Chance, K., Kurosu, T., Guenther, A., Wiedinmyer, C., Stanton, J., Pilling, M., Pressley, S., Lamb, B., & Sumner, A. L. (2006). Quantifying the seasonal and interannual variability of North American isoprene emissions using satellite observations of formaldehyde column, *J. Geophys. Res.*, **111**, D12315, doi:10.1029/2005JD006689.
5. Fu, T.-M., Jacob, D. J., Palmer, P. I., Chance, K., Wang, B.Y., Barletta, X., Blake, D. R., Stanton, J. C., & Pilling, M. J. (2007). Space-based formaldehyde measurements as constraints on volatile organic compound emissions in East and South Asia, *J. Geophys. Res.*, **112**, D06312, doi:10.1029/2006JD007853.
6. Stavrakou, T., Müller, J.-F., De Smedt, I., Van Roozendael, M., van der Werf, G.R., Giglio, L. & Guenther, A. (2009). Global emissions of non-methane hydrocarbons deduced from SCIAMACHY formaldehyde columns through 2003-2006, *Atmos. Chem. Phys.,* **9**, 3663-3679.
7. Myriokefalitakis, S., Vrekoussis, M., Tsigaridis, K., Wittrock, F., Richter, A., Brühl, C., Volkamer, R., Burrows, J. P. & Kanakidou, M. (2008). The influence of natural and anthropogenic secondary sources on the glyoxal global distribution, *Atmos. Chem. Phys.*, **8**, 4965–4981.
8. Vrekoussis, M., Wittrock, F., Richter, A. & Burrows, J. P. (2009). Temporal and spatial variability of glyoxal as observed from space, *Atmos. Chem. Phys.*, **9**, 4485-4504.
9. Fu, T.M., Jacob, D.J., Wittrock, F., Burrows, J.P., Vrekoussis, M. & Henze D.K. (2008). Global budgets of atmospheric glyoxal and methylglyoxal, and implications for formation of secondary organic aerosols, *J. Geophys. Res.*, **113**, D15303, doi:10.1029/2007JD009505.
10. Hallquist, M., Wenger, J.C., Baltensperger, U., Rudich, Y., et al. (2009). The formation, properties and impact of secondary organic aerosol: current and emerging issues, *Atmos. Chem. Phys.*, **9**, 5155-5236.
11. Munro, R., Eisinger, M., Anderson, C., Callies, J., Corpaccioli, E., Lang, R., Lefebvre, A., Livschitz, Y., & Albiñana, A. P. (2006). GOME-2 on MetOp, in: *Proc. of The 2006 EUMETSAT Meteorological Satellite Conference*, Helsinki, Finland, 12–16 June, EUMETSAT P.48.
12. Platt, U. & Stutz, J. (2008). Differential Optical Absorption Spectroscopy: Principles and Applications. *Physics of Earth and Space Environments,* Ed. Springer, 3540211934, 9783540211938.
13. Grainger, J.F. & Ring, J. (1962). Anomalous Fraunhofer line profiles, *Nature*, **193**, 762.
14. Chance, K. & Spurr, R., (1997). Ring effect studies: Rayleigh scattering including molecular parameters for rotational Raman scattering, and the Fraunhofer spectrum, *Appl. Optics*, **36**, 5224–5230.
15. Kylling, A. & Mayer, B. (2003). LibRadTran: A package for UV and visible radiative transfer calculations in the Earth's atmosphere, http://www.libradtran.org.
16. Wang, P., Stammes, P., van der A, R., Pinardi, G., & van Roozendael, M., (2008). FRESCO+: an improved O2 A-band cloud retrieval algorithm for tropospheric trace gas retrievals, *Atmos. Chem. Phys.*, **8**, 6565–6576.
17. Richter, A. & Wagner, T., (2001). Diffuser plate spectral structures and their influence on GOME slant columns, *Technical note*.
18. De Smedt, I., Müller, J.-F., Stavrakou, T., van der A, R., Eskes, H. & Van Roozendael, M. (2008). Twelve years of global observation of formaldehyde in the troposphere using GOME and SCIAMACHY sensors, *Atmos. Chem. Phys.*, **8**, 4947–4963.
19. Wittrock F., Richter, A., Oetjen, H., Burrows, J. P., Kanakidou, M., Myriokefalitakis, S., Volkamer, R., Beirle, S., Platt, U., & Wagner, T. (2006). Simultaneous global observations of glyoxal and formaldehyde from space, *Geophys. Res. Lett.*, **33**, L16804, doi:10.1029/2006GL026310.
20. Kurosu, T.P., Chance, K., Liu, X., Volkamer, R., Fu, T.M., Millet, D., Jacob, D.J. & Levelt, Pieternel (2007). Seasonally resolved global distributions of glyoxal and formaldehyde observed from the Ozone Monitoring Instrument on EOS Aura, in: *Proc. of Anais XIII Simpósio Brasileiro de Sensoriamento Remoto*, Florianópolis, Brasil, 21-26 April 2007, 6461-6464.
21. Pope, R.M. & Fry, E. S., (1997). Absorption spectrum (380-700 nm) of pure water. II. Integrating cavity measurements, *Appl. Opt.*, **36**, 8710-8723.